# Optimizing the Design of the Landing Slope of the Zao Jumping Hill

Kazuya Seo[1], Yuji Nihei[2], Toshiyuki Shimano[3], Ryutaro Watanabe[2] and Yuji Ohgi[4]
[1]*Department of Education, Art and Science, Yamagata University, 1-4-12 Kojirakawa, Yamagata, Japan*
[2]*Yamagata City Office, 2-3-25 Hatagomachi, Yamagata, Japan*
[3]*Access Corporation, 2-3-4, Minami-1-jo Higashi, Chuo-ku, Sapporo, Japan*
[4]*Graduate School of Media and Governance, Keio University, 5322 Endo, Fujisawa, Japan*

Keywords: Optimal Design, Ski Jumping, Landing Slope, Flight Dynamics, Safety Landing, Construction Fee, Variety.

Abstract: This paper describes a process for optimizing the design of the landing slope of the Zao jumping hill. The features of the landing slope that we considered were the construction fee, the safety of the jumpers on landing, the length of the flight distance such that it makes it an interesting spectacle, and the difficulty for unskilled jumpers. We regard these features as objective functions. The findings can be summarized as follows: it is possible to control the four objective functions by changing the profile of the landing slope; the safety on landing is almost equivalent to the difficulty for unskilled jumpers; there is a trade-off between the length of the flight distance and the safety on landing and the difficulty for unskilled jumpers; the construction fee is influenced by the horizontal distance between the edge of the take-off table and the K-point; and the safety on landing, the flight distance and the difficulty for unskilled jumpers are influenced by the ratio of the height difference and the horizontal distance between the edge of the take-off table and the K-point.

## 1 INTRODUCTION

Since 2012 the Zao jumping hill in Yamagata city has been host to the annual ladies world cup. A ski jumping hill is composed of the in-run, the take-off table, the landing slope and the out-run. The Zao track was renovated to resemble the ski jump at the Sochi Games in 2013, with a take-off table with an angle of 11 degrees downhill. A further renovation related to the landing slope is being planned for 2015, and this is the subject of this study. It is likely to cost 700,000,000 Japanese yen (5,800,000 USD, or 5,000,000 EUR), so there is a huge responsibility on the shoulders of the authors.

The concept behind the design of the landing slope is that the landing slope should enable the spectators to witness an exciting spectacle, that the jumpers land safely, and that it be constructed with the minimum cost.

## 2 OBJECTIVE FUNCTIONS

A long flight ditance provides an exciting spectacle for the spectators. The first objective function for the Zao jumping hill is the flight distance; the longer the flight distance, the more exciting the spectacle.

On the other hand, the landing slope in Zao is designed to be a difficult slope for unskilled jumpers, which means it will not produce long flight distances for unskilled jumpers. This is the concept of the second objective function.

The construction fee was estimated on the basis of the amount of material that is needed to construct the new slope. Some of this material will be moved from the existing Zao jumping hill, while new material will also have to be brought in. Lower cost is, of course, better.

The safety on landing was estimated on the basis of the landing velocity. The landing velocity is the velocity component perpendicular to the landing slope at the instance of landing, and this needs to be small to reduce the impact and make the landing safer.

### 2.1 Construction Fee

The construction fee was estimated on the basis of the amount of material needed to construct the new slope. This is the first objective function, *F1*.

The inertial coordinate system is shown in Figure



Seo, K., Nihei, Y., Shimano, T., Watanabe, R. and Ohgi, Y..
Optimizing the Design of the Landing Slope of the Zao Jumping Hill.
In *Proceedings of the 3rd International Congress on Sport Sciences Research and Technology Support (icSPORTS 2015)*, pages 208-213
ISBN: 978-989-758-159-5

1. The origin is defined as being at the edge of the take-off table, while the $X_E$-axis is in the horizontal forward direction and the $Z_E$-axis is vertically downward. The height difference between the old Zao and the new Zao at $X_E$ is denoted by $h(X_E)$ as shown in Figure 2. The width at $X_E$ is denoted by $b(X_E)$. The amount of material needed to construct the new jumping hill is derived using equation (1).

$$Amount\ of\ material : \int_0^{132} |h(X_E)| \cdot b(X_E) dX_E \quad (1)$$

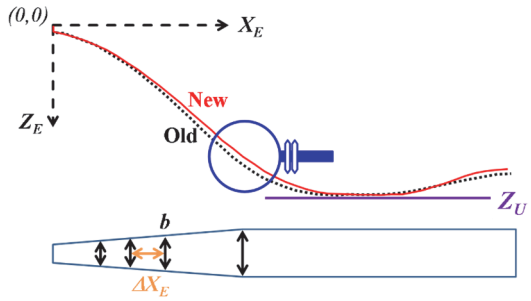


Figure 1: Inertial coordinate system.

The landing profiles of the old and the new Zao.

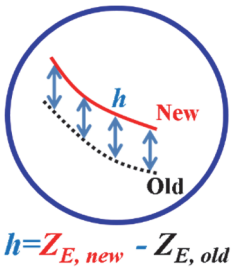


Figure 2: Height difference between the old and the new Zao.

The construction fee depends on the height to which material needs to be taken to construct the new hill. The greater the height, the more expensive the construction fee. Here, the lowest cost is at $Z_U$ (at the bottom of the slope) and this is assumed to be 200 Japanese yen per 1 $m^3$, while the highest cost is at $Z_E$=0 (at the top of the slope), which is assumed to be 10,000 yen per 1 $m^3$ on the basis of experience. The cost between $Z_U$ and $Z_E$=0 is derived using a linear relationship between cost and height. Therefore, the construction fee, *F1*, can be estimated using equation (2).

$$F1 = \int_0^{132} |h(X_E)| \cdot b(X_E) \cdot \left\{ -\frac{9800}{Z_U} (Z_E(X_E) - Z_U) + 200 \right\} dX_E \quad (2)$$

## 2.2 Safety Landing

The safety on landing was estimated on the basis of the landing velocity (McNeil et al., 2012). In order to estimate the landing velocity, the flight trajectory needs to be simulated. This is discussed in section 3. The landing velocity is the velocity component perpendicular to the landing slope at the instance of landing (Figure 3), and this needs to be small to reduce the impact and make the landing safer. The landing velocity, *F2*, is shown in equation (3), where the flight path angle and the slope of the landing hill at the landing point are denoted by $\gamma$ and $\beta_H$.

$$F2 = v_\perp = V \sin(\gamma - \beta_H) \quad (3)$$

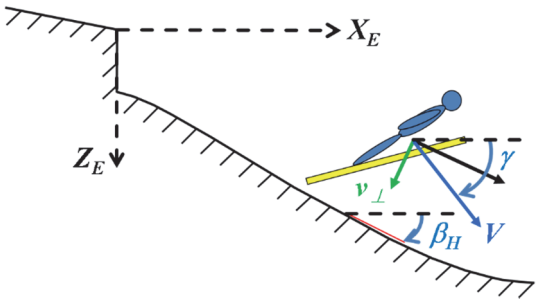


Figure 3: Landing velocity, $v_\perp$.

## 2.3 Flight Distance

A ski jumping hill should be designed so that it contributes to the creation of an exciting spectacle, which means that the jumpers have longer flight distances. The flight distance is defined by the distance along the profile of the landing slope. *F3*, which is the flight distance multiplied by -1, is obtained from equation (4). The flight trajectory needs to be simulated in order to determine the landing point, $X_E(tf)$. Here, the flight time is denoted by *tf*. This is discussed in section 3.

$$F3 = -\int_0^{X_E(tf)} \sqrt{\left(X_E^{\ 2} + Z_{E,new}^{\ 2}\right)} dX_E \quad (4)$$

## 2.4 Difficulty for Unskilled Jumpers (Variation in the Flight Distance)

The landing slope in Zao is designed to be a difficult slope for unskilled jumpers. The flight distances of unskilled jumpers are less than those of skilled jumpers because they are unable to satisfy the optimal conditions from take-off through to landing. Therefore, a landing slope for which the variance in the flight distance is large is defined as a difficult slope for unskilled jumpers.

The variance in the flight distance multiplied by -1, *F4*, is defined by equation (5), where $FD_L$ is the local longest flight distance, shown by × in Figure 4, $FD_i$ are simulated flight distances around $FD_L$, shown by ●, and $n$ is the number of flight simulations. The abscissa and the ordinate in Figure 4 are design variables, which are the angles given in #7 through #22 in Table 1. The ellipse in Figure 4 corresponds to the human error.Since the jumper is not a robot, there will be some human error, which shortens the flight distance. The human error is assumed to be 2° for all angles from #7 through #22. Fifty Monte-Carlo simulations (i.e. $n$=50) were carried out to estimate *F4*.

$$F4 = -\sqrt{\frac{\sum_{i=1}^{n}(FD_i - FD_L)^2}{n-1}} \tag{5}$$

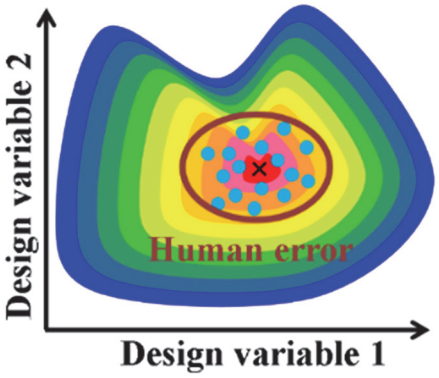


Figure 4: Contour map of flight distance. $FD_L$: Longest flight distance shown by ×, $FD_i$: Flight distances around $FD_L$ shown by ●.

## 3 FLIGHT SIMUULATION

In order to estimate *F2*, *F3* and *F4*, the flight trajectory needs to be simulated. It is assumed that the motion of the body–ski combination occurs in a fixed vertical plane. The coordinate system for the body is shown in Figure 5. The origin is defined as the center of gravity of the body–ski combination.

In terms of coordinate transformations (Stevens and Lewis, 2003) we then have

$$\dot{X}_E = U\cos\Theta + W\sin\Theta \tag{6}$$

$$\dot{Z}_E = -U\sin\Theta + W\cos\Theta \tag{7}$$

Here, ($U$, $W$) are the ($x_b$, $z_b$) components of the velocity vector. The equations of motion and the moment equation are

$$\dot{U} = \frac{1}{m}[X_a - mg\sin\Theta] - QW \tag{8}$$

$$\dot{W} = \frac{1}{m}[Z_a + mg\cos\Theta] + QU \tag{9}$$

$$\dot{Q} = \frac{M_a}{I_{yy}} \tag{10}$$

$$\dot{\Theta} = Q \tag{11}$$

Here, ($X_a$, $Z_a$) are the ($x_b$, $z_b$) components of the aerodynamic force, $Q$ is the $y_b$ component of the angular velocity vector, $m$ is the mass of the body–ski combination, $g$ is the gravitational acceleration, $M_a$ is the $y_b$ component of the aerodynamic moment, and $I_{yy}$ is the moment of inertia of the body–ski combination on the $y_b$-axis. The flight trajectory ($X_E(t)$, $Y_E(t)$, $Z_E(t)$) can be obtained by integrating Equations (6) through (11) numerically.

The aerodynamic forces $X_a$ and $Z_a$ in Equations (8) and (9) are derived from $D$ and $L$ as given in Eqns. (12) and (13).

$$X_a = L\sin\alpha - D\cos\alpha \tag{12}$$

$$Z_a = -L\cos\alpha - D\sin\alpha \tag{13}$$

The aerodynamic drag and lift and moment in Eqns. (10), (12) and (13) were all obtained during wind tunnel tests as functions of α, β and λ (Seo, Watanabe and Murakami, 2004). The wind tunnel data were acquired for α at 5° intervals between 0° and 40°, and for β at intervals of 10° between 0° and 40°. The ski-opening angle λ was set at either 0°, 10° or 25°. The torso and legs of the model were always set in a straight line. The tails of the skis were always in contact on the inner edges.

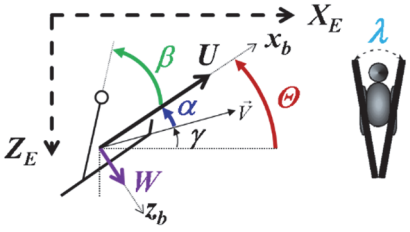


Figure 5: Coordinate system for the body and definition of characteristic parameters.

## 4 DESIGN VARIABLES

The 22 design variables are shown in Table 1. The first six are concerned with the landing slope (Figure 6), while the other 16 are concerned with various angles of the jumper during the jump. The time variations of β and λ are estimated on the basis of

the spline curves, which are constructed from the control points, #9 through 22, in Table 1. The take-off table is at an angle of 11 degrees downhill and the hill size (HS) is set at 106 meters, following a request from Yamagata city hall. The mass of the body-ski combination is assumed to be 50 kg, the take-off speed along and perpendicular to the take-off table are assumed to be 24.55 m/s and 2 m/s, respectively.

Optimization was carried out with the aid of a genetic algorithm (GA). The 'ranges for GA', which are also shown in Table 1, are defined such that they cover practical values.

In the optimization process, all the objective functions, from *F1* through *F4*, should be minimized. The optimization is to determine which set of design variables makes all the objective functions smallest.

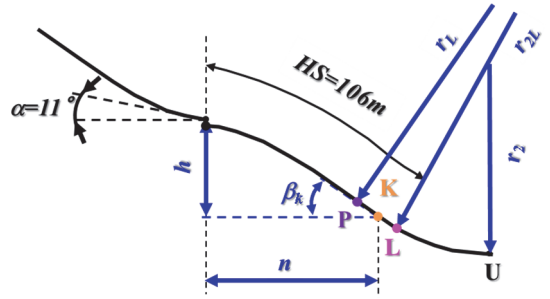


Figure 6: Landing slope and design variables.

Table 1: Design variables.

| # | Design variables | Ranges for GA |
|---|---|---|
| 1 | $n$ | 70～90 m |
| 2 | $\beta_k$ | 30～35 ° |
| 3 | $r_L$ | 200～240 m |
| 4 | $r_2$ | 80～100 m |
| 5 | $r_{2L}$ | 80～100 m |
| 6 | $h/n$ | 0.541～0.543 |
| 7 | $\Theta_0$ | -11～10 ° |
| 8 | $Q_0$ | -40～10 °/s |
| 9 | *β at 0.3sec.* | 20～38 ° |
| 10 | *β at 1.3sec.* | 2～38 ° |
| 11 | *β at 2.3sec.* | 2～38 ° |
| 12 | *β at 3.3sec.* | 2～38 ° |
| 13 | *β at 4.3sec.* | 2～38 ° |
| 14 | *β at 5.3sec.* | 2～38 ° |
| 15 | *β at 6.3sec.* | 2～38 ° |
| 16 | *λ at 0.3sec.* | 2～28 ° |
| 17 | *λ at 1.3sec.* | 2～28 ° |
| 18 | *λ at 2.3sec.* | 2～28 ° |
| 19 | *λ at 3.3sec.* | 2～28 ° |
| 20 | *λ at 4.3sec.* | 2～28 ° |
| 21 | *λ at 5.3sec.* | 2～28 ° |
| 22 | *λ at 6.3sec.* | 2～28 ° |

# 5 CONSTRAINTS

Due to financial reasons, the amount of material needed to reconstruct the Zao jumping hill was limited to

- less than 1.0 meters at $X_E$=45
- less than 2.0 meters at $X_E$=80
- less than 2.0 meters at $X_E$=131.9 (old U point)

Moreover, α, $\beta$ and λ (Figure 5) were limited by the experimental ranges, as follows.

- 0°< α <40°
- 0°< $\beta$ <40°
- 0°<λ<30°

Finally, only flight distances of more than 84 meters were considered.

# 6 RESULTS AND DISCUSSIONS

Self-organizing maps (SOM) of the objective functions are shown in Figure 7. These are contour maps colored by each objective function value. Blue denotes the lowest value, while red denotes the highest. A SOM is useful for enabling low-dimensional views of high-dimensional data (Kohonen, 1995).

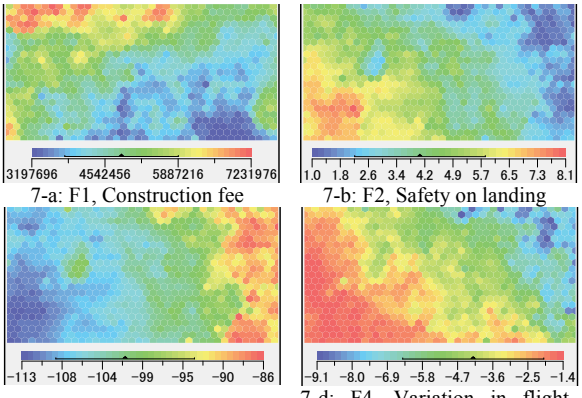


7-a: F1, Construction fee

7-b: F2, Safety on landing

7-c: F3, Flight distance

7-d: F4, Variation in flight distance

Figure 7: Self-organizing maps of the objective functions.

It can be seen from Figures 7-b and 7-d that the color patterns of the contour maps are almost same. Therefore, it can be concluded that the safety on landing (*F2*) is almost equivalent to the difficulty for unskilled jumpers (variation in flight distance, *F4*). The safest landing is where the gradient of the landing slope at the landing point is almost parallel to that of the flight trajectory of the jumper. On the

other hand, the same gradient for the flight trajectory and the landing slope at the instance of landing gives a larger variation in flight distance. This is the reason why the safety on landing (*F2*) is almost equivalent to the difficulty for unskilled jumpers (*F4*).

On the other hand, the contour maps of Figures 7-b and 7-d are almost the converse of that in Figure 7-c. This means that there is a trade-off between the flight distance (Figure 7-c) and the other two objective functions (Figures 7-b & 7-d). Although the lowest values for all the objective functions gives the ideal situation, it is impossible to meet this criterion. This is because the four objective functions conflict with one another. The extreme case of the longest flight distance is located at the bottom left hand side of the SOM, where Figure 7-c shows the lowest value and Figures 7-b and 7-d show almost their highest values. The landing slope that produces the longest flight distance gives the worst safety on landing (dangerous landing) and is the most difficult for unskilled jumpers (the difference in flight distance between skilled and unskilled jumpers is small).

The contour map of Figure 7-a is completely different from the other three maps (Figure 7-b, 7-c & 7-d). The color gradient of Figure 7-a is in the transverse direction, while the color gradients of the other three maps are in the lateral direction.

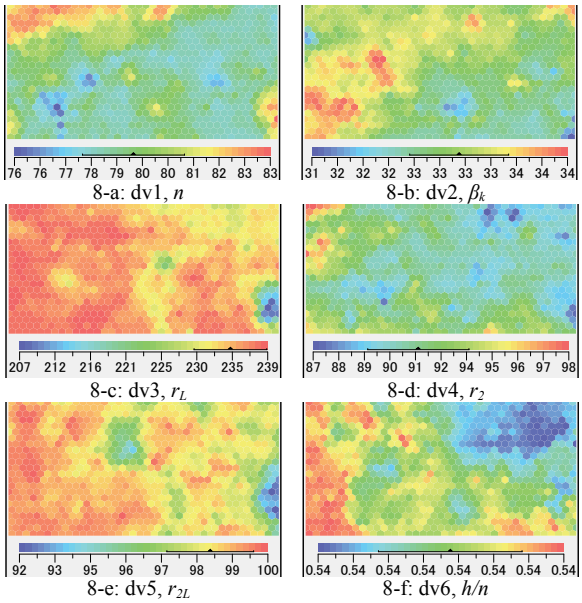


Figure 8: Self-organizing maps of design variables concerned with the landing slope.

Self-organizing maps for the 6 design variables concerned with the landing slope are shown in Figure 8. It can be seen that the color pattern of Figure 8-f is almost the same as those of Figures 7-b and 7-d, while it is almost the converse of that in Figure 7-c. This means that the three objective functions, *F2*, *F3* and *F4* are influenced by *h/n*. It is self-evident that the smaller *h/n* makes the flight distance shorter, and vice versa.

The color gradient of Figure 8-a, *n*, is in the transverse direction, as in Figure 7-a. This means that *F1* is influenced by *n*.

The color patterns of the other four design variables in Figure 8 do not match those in Figure 7. Therefore, these four design variables, $\beta_k$, $r_L$, $r_2$, $r_{2L}$, do not affect the objective functions.

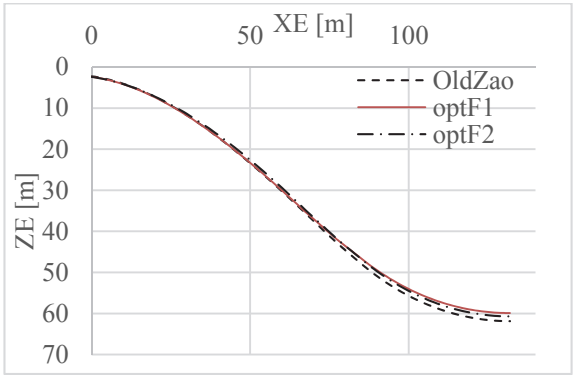


Figure 9: Comparison between the old Zao landing slope and two examples.

Extreme examples of landing slopes are shown in Figure 9. The broken line shows the profile of the old Zao landing slope, the solid line shows the profile of the lowest cost landing slope (optF1) and the dash-dot line shows the profile which produces the safest landing (optF2). It is possible to control the construction fee, the flight distance and so on, by changing the profile of the landing slope. The profile of the low cost slope coincides with the old profile especially at greater height (around $Z_E$=10), though the profile is different at lower levels (around $Z_E$=50).

On the other hand, the slope with the safest landing (optF2) is steeper around $X_E$ =70. This steeper slope tends to coincide with the flight trajectory. Therefore, the velocity component perpendicular to the landing slope is small. The solid line (optF1) comes close to the dash-dot line (optF2) at around $X_E$ =70.

Other, more extreme, examples of landing slopes are shown in Figure 10. The profile which produces the longest flight distances (optF3) is almost the same as that of the most difficult case (optF4) at $X_E$ =40, while it is lower at $X_E$ =80. Since the flight distance

is defined by the distance along the profile, as given by equation (4), the profile of the solid line produces longer flight distances for the same trajectory.

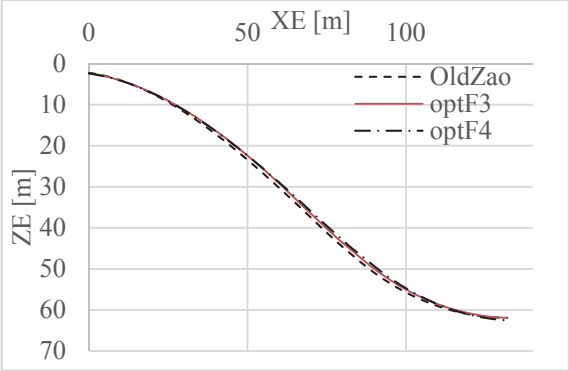


Figure 10: Comparison between the old Zao landing slope and two examples.

## 7 CONCLUDING REMARKS

Optimization of the design of the landing slope was carried out. The content of the paper is summarized as follows:

- Four objective functions, which are the construction fee, the safety on landing, the flight distance and the difficulty for unskilled jumpers, were considered.
- It is possible to control the four objective functions by changing the profile of the landing slope.
- Safety on landing is almost equivalent to the difficulty for unskilled jumpers (variation of flight distance around the local longest flight distance).
- There is a trade-off between long flight distance and the safety on landing and the difficulty for unskilled jumpers.
- The construction fee is influenced by $n$ (the horizontal distance between the edge of the take-off table and the K-point).
- The safety on landing, the flight distance and the difficulty for unskilled jumpers are influenced by $h/n$, the ratio of the height difference and the horizontal distance between the edge of the take-off table and the K-point.

## ACKNOWLEDGEMENTS

This work is supported by a Grant-in-Aid for Scientific Research (A), No. 15H01824, Japan Society for the Promotion of Science.

## REFERENCES

Kohonen T., 1995. *Self-Organizing Maps*, Springer, Berlin, Heidelberg.

McNeil A. J., Hubbard M. and Swedberg, A. D., 2012. Designing tomorrow's snow park jump, *Sports Engineering*, 15, 1-20

Stevens B. and Lewis F., 2003. *Aircraft control and simulation*, Wiley, Hoboken, New Jersey, 2nd edition.

Seo K., Watanabe I. and Murakami M., 2004. Aerodynamic force data for a V-style ski jumping flight. *Sports Engineering,* 7, 31-39.